Proceedings IRF2018: 6th International Conference Integrity-Reliability-Failure
Lisbon/Portugal 22-26 July 2018. Editors J.F. Silva Gomes and S.A. Meguid
Publ. INEGI/FEUP (2018); ISBN: 978-989-20-8313-1

PAPER REF: 7128

MODELLING OF THE MECHANICAL RESPONSE OF Zr-Nb AND Ti-Nb ALLOYS IN A WIDE TEMPERATURE RANGE

Vladimir A. Skripnyak[1(*)], Vladimir V. Skripnyak[1], Evgeniya G. Skripnyak[1], Nataliya V. Skripnyak[1,2]
[1]National Research Tomsk State University, Tomsk, Russia
[2]Linköping University, Linköping, Sweden
[(*)]*Email:* skrp2006@yandex.ru

ABSTRACT

This article presents the results of modelling of the mechanical behaviour of biocompatible Zr-Nb and Ti-Nb alloys in the range of strain rates from 10^{-3} to 10^{3} s^{-1} at temperatures from 297 K to 1273 K. Modification of the micro-dynamical model was proposed for the description of Zr-1Nb ultrafine grained and coarse grained alloys. It was shown that the phase transition HCP → BCC alloy Zr-Nb at elevated temperatures leads to a sharp changing in the resistance to plastic flow and kinetics of growth of damage. The results can be used for engineering analysis of designed constructive elements of technical and biomedical applications.

Keywords: ductility, fracture, elevated temperature, zirconium alloys, titanium alloys.

INTRODUCTION

Improvement in the technology of fabrication of some constructional elements for nuclear reactors is connected with computer simulation of mechanical properties and structural evolution of radiation-resistant alloys Zr-Nb (Rodchenkov, 20005; Motta, 2007; Blokhin, 2011). In this regard, there is an increasing need to develop computational models of the mechanical behaviour of advanced Zr-Nb in loading conditions close to operating ones. The Zr-Nb has a unique complex of physical and mechanical properties and is considered as promising structural alloys for nuclear reactors of IV generation (Blokhin, 2011). Coarse grained (CG) and ultrafine grained (UFG) zirconium alloys with a concentration of Nb below 2.5 weight % and additionally doped with Mo, Fe, Cr for the stabilization of precipitations of beta-phase Zr were studied during last decade (Fong, 2013). It is known that the formation of ultrafine-grained structures in the alloys of Zr-Nb not only improves the yield and strength of the alloy, but also prevents the formation of cracks at the mesoscopic level (Behera, 2016).

Last years Ti-Nb-Zr alloys were developed and studied. These alloys have remarkable properties such as low density, high melting point, good oxidation resistance and high specific strengths, low elastic moduli, biocompatibility, etc. (Nikonov, 2015; Bobbili, 2017). Understanding of the mechanical behavior of Ti-Nb-Zr alloys in a wide temperature range is extremely essential for the numerical modeling of various applications and manufacturing technologies.

In this connection, the mechanical behavior of Zr-1%Nb alloy was studied by numerical simulation method in the practically important temperature range from 297 K to 1243 K. Mechanical behavior of Ti-13Nb-13Zr alloy simulated within practically important temperature range from 297 K to 1050 K.

COMPUTATIONAL MODEL

The numerical models for simulation of the tensile tests were developed using the licensed ANSYS 14.5 software and Autodyn software. Numerical solution of this problem allows to investigate the adequacy of prediction of mechanical behavior of alloys Zr1 % Nb and Ti-13Nb-13Zr when using the modified Johnson-Cook and Zerilli-Armstrong constitutive equations.

Mechanical behavior of specimens was described by a system of conservation equations (mass, momentum and energy), kinematic equation and the constitutive equation. Mechanical behavior of specimens was described by a system of conservation equations (mass, momentum and energy), kinematic equation and the constitutive equation.

Initial and boundary conditions corresponded to uniaxial tension of specimens (Skripnyak, 2016). Dog bone shape specimens were simulated under axial tension with a constant strain rate (Skripnyak, 2017).

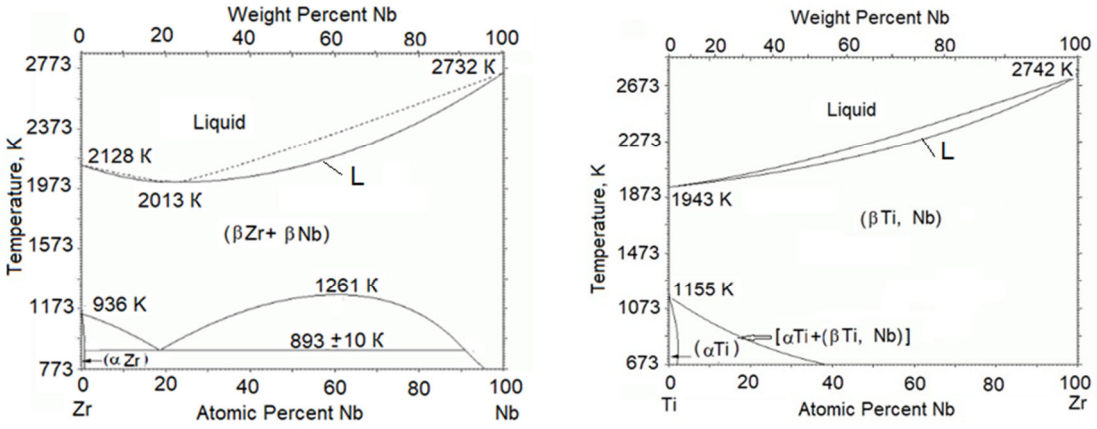

(a) (b)

Fig. 1 - (a) Binary phase diagram of Zr-Nb alloy (Clouet,2018); (b) Binary phase diagram of Ti-Nb alloy (Hatt, 1968; Moffat,1988; Bonisch, 2013)

The calculations were carried out using solvers on finite-difference scheme of second order accuracy. Plastic flow was described within the theory of Prandtl-Reuss with the criterion of von Mises.

The phase structure of Zr-Nb and Ti-Nb alloys changes from duplex α+β to single β phase structure at deformation temperatures above temperature of α → β transition. Alpha phases of Zr-Nb and Ti-Nb alloys have a hexagonal close packed (HCP) crystal structure. Beta phases of these alloys have body centered cubic (BCC) crystal structure (Nikonov, 2015; Bonisch, 2013; Eckert, 2013). Therefore, the flow stress of zirconium alloys under loading can be described using a modification of Johnson-Cook model (1) and Zerilli-Armstrong model for α-phase alloy (2) and β-phase alloy with a body centered cubic (BCC) crystal structure (3) (Johnson, 1985; Zerilli, 1992; Gao, 2011; Abed, 2005):

$$\sigma_s(\varepsilon^p_{eq}, \dot{\varepsilon}_{eq}, T) = (a + k_h d_g^{-1/2} + b(\varepsilon^p_{eq})^n)(1 + c\ln(\dot{\varepsilon}_{eq}/\dot{\varepsilon}_0))(1 - \bar{T}^m), \quad (1)$$

$$\sigma_s(\varepsilon^p_{eq}, \dot{\varepsilon}_{eq}, T) = [C_0 + k_h d_g^{-1/2} + C_5(\varepsilon^p_{eq})^{n_1}]\exp\left(C_4 T \ln(\dot{\varepsilon}_{eq}/\dot{\varepsilon}_0)\right)\{1 - [-C_3 T\ln(\dot{\varepsilon}_{eq}/\dot{\varepsilon}_0)]^q\}^p, \quad (2)$$

$$\sigma_s(\varepsilon^p_{eq}, \dot{\varepsilon}_{eq}, T) = C_0 + k_h d_g^{-1/2} + C_1\exp\left(-C_3 T + C_4 T \ln(\dot{\varepsilon}_{eq}/\dot{\varepsilon}_0)\right) + C_5(\varepsilon^p_{eq})^{n_1}, \text{ for BCC alloys} \quad (3)$$

where $\varepsilon_{eq}^{p}=[(2/3)\varepsilon_{ij}^{p}\varepsilon_{ij}^{p}]^{1/2}$, $\dot{\varepsilon}_{eq}=[(2/3)\dot{\varepsilon}_{ij}\dot{\varepsilon}_{ij}]^{1/2}$, $\dot{\varepsilon}_{0}=1.0\,s^{-1}$, a, b, c, n, m are the material parameters, T is the temperature, $\overline{T}=(T-T_r)/(T_m-T_r)$, Tr =295 K is room temperature, T_m is the melting temperature, k_h is the coefficient of the Hall−Petch relation, C_0, C_1, C_3, C_4, C_5, n_1, q, p are material constants, d_g is the grain size.

The melting temperature T_m of alloy depends on the weight concentration of components. The melting temperature of Zr-Nb and Ti-Nb alloys versus weight concentration of Nb are represented by the liquidus curves (L) in Figures 1(a) and (b), respectively.

The calculations were performed for the alloy E110 (Zr-1Nb) with the average grain size of 7 microns in the range of plastic deformation from 0 to 14 % and temperature in the range from 297 K to 1173 K. The values for the parameters of the Johnson-Cook model are shown in Table 1. The values for the material parameters of the modified Zerilli-Armstrong model are shown in Table 2. Tm was assumed equal to 2128 K.

Table 1 - Material parameters of Johnson-Cook model

Alloy	a (MPa)	k_h (MPa μm$^{1/2}$)	b (MPa)	n	m	c
Zr-1Nb	290	368 for 1.1 μm<dg<100 μm	386	0.11	0.6 at T< 1070 K 0.14 at T> 1070 K	0.14
Zr-1Nb	625	40 for 0.08 μm<dg<1.1 μm	386	0.11	0.21 at T< 1070 K 0.14 at T> 1070 K	0.14
Ti-13Nb-13Zr	680	199 for 1.1 μm<dg<60 μm	960	0.3	0.71 at T< 1050 K	0.015

Table 2 - Material parameters of Zerilli-Armstrong model

Alloy	C_0 (MPa)	k_h (MPa μm$^{1/2}$)	C_1 (MPa)	C_3 (1/K)	C_4 (1/K)	C_5 (MPa)	n_1	q	p
Zr-1Nb	110	368 for 1.1 μm<dg<100 μm	-	0.00807 at T< 1070 K	0.000395	405	0.19	2/3	2
Zr-1Nb	445	63 for 0.08 μm<dg<1.1 μm	1015	0.00807 at T< 1070 K	0.000395	405	0.19	-	-
Ti-13Nb-13Zr	680	199 for 1.1 μm<dg<60 μm	-	0.00807 at T< 1050 K	0.000395	960	0.3	2/3	2

RESULTS AND DISCUSSION

Figure 2 shows the calculated stress - strain curves of Zr-1Nb-1Sn alloy under uniaxial tension at strain rate of 10^{-3} s^{-1}. Solid black curves indicate experimental true stress versus true strain curves (Xiao, 2010; Sarkar, 2017). Colored and dashed curves were obtained using equation (2) and (1) respectively. The model of Zerilli-Armstrong describes the change of the strain hardening in the temperature range more adequately in comparison with the Johnson-Cook model.

Figure 3 shows normalized yield strength versus normalized temperature under tension at strain rate 1 s^{-1} for the Zr-1Nb - 1Sn alloy. The change in the slope of the curve $\sigma_s/\sigma_0(\overline{T})$ indicates a change in the physical mechanisms that ensure the development of plastic deformations. The good agreement of the calculation results with the experimental data on the resistance of plastic deformation of the alloy Zr-1Nb - 1Sn in the temperature range from 295 to 1173 K was obtained under the assumption of changing the numerical values of the material parameters at temperatures above 1070 K.

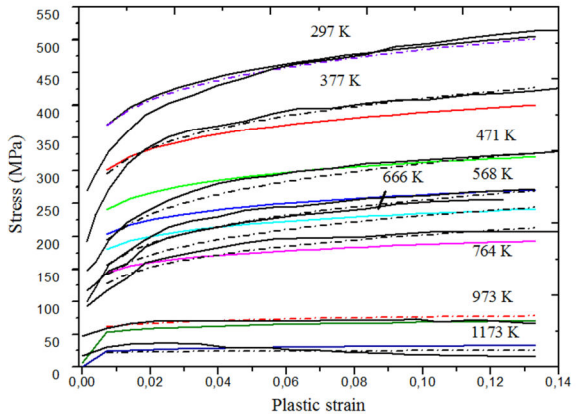

Fig 2 - Calculated stress versus plastic strain of Zr-1Nb-1Sn alloy at the tensile strain rate of 10^{-3} s^{-1}, black solid curves corresponds to experimental data (Xiao, 2010; Sarkar, 2017)

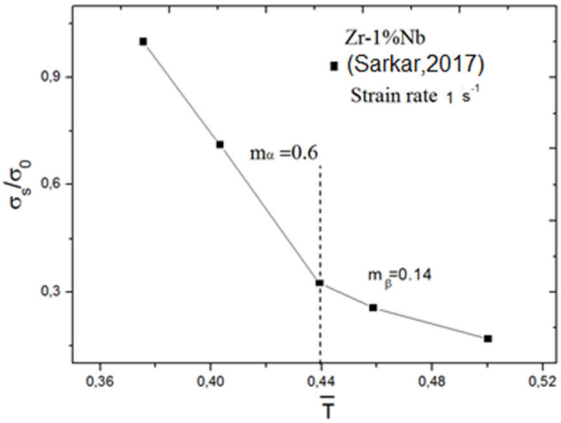

Fig 3 - Normalized yield strength versus normalized temperature under tension at strain rate 1 s^{-1} for the Zr-1%Nb alloy. Symbols are experimental data (Sarkar, 2017)

The marked change is due to the change in the phase composition of the alloy at a temperature above ~1070 K. It should be noted that the calculations were performed in the strain rate range from 10^{-3} to 10 s^{-1}. Constitutive equations should be amended from (2) to (3) if the temperature exceeds the temperature of beginning of phase transformations, $\alpha \rightarrow \beta$ (~1070 K).

Figure 4 shows the calculated stress versus strain curves of Ti-13Nb-13 Zr alloy at the tensile strain rate of 10^{-2} s^{-1}. Results of simulation agree with experimental data within temperature range from 298 K to 873 K. In this temperature range, the Ti-13Nb-13Zr alloy remains two-phase. In this temperature range, the Ti-13Nb-13Zr alloy remains two-phase. In this case, the numerical values of the material parameters in the constitutive equation (2) are not changed significantly and these parameters can be considered as constants.

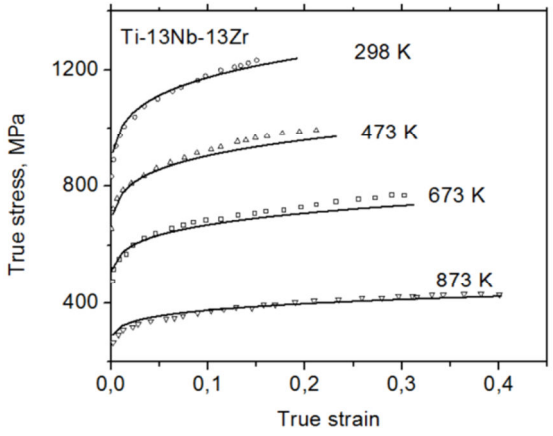

Fig. 4 - Calculated stress versus strain of Ti-13Nb-13Zr alloy at the tensile strain rate of 10-2 s-1. Symbols are experimental data (Bobbili, 2017)

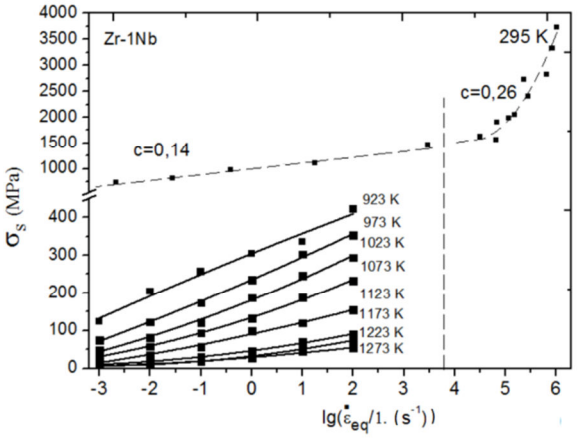

Fig. 5 - Normalized yield strength versus logarithm of normalized strain rate under tension for the samples of the Zr-1 % Nb alloy. Experimental data from Xiao, 2010, Kazakov, 2015 and Sarkar, 2017)

Figure 5 displays results of simulation of the yield strength versus logarithm of normalized strain rate under tension of the Zr-Nb. The average grain size was 15 μm. Solid curves calculated in the temperature range from 295 K to 1273 K and range of strain rates range from 10^{-3} s^{-1} to 10^{2} s^{-1}. The dashed curve calculated at the room temperature, and range of strain rates from 10^{-3} to 10^{6} s^{-1}. Experimental data (Xiao, 2010; Kazakov, 2015; Sarkar, 2017) are shown by filled symbols.

Thus, it was shown that the dependence of the yield strength of the Zr-1Nb alloy on the logarithm of normalized strain rate is close to linear in the temperature range from 297 K to 1273 K and strain rates from 10^{-3} to 10^{2} s^{-1}. Both constitutive equations (1)-(3) allow obtaining satisfactory predictions of the yield stress under tension in the range of strain rates from 10^{-3} to ~10^{3} s^{-1} and temperature from 297 K to temperature of phase transition $T_{\alpha\rightarrow\beta}$.

It was found, that it is necessary to change the numerical value of the coefficient c in constitutive equations (1) to obtain a satisfactory agreement of calculated yield strength with experimental data (Kazakov, 2015). Calculated stress - strain curves of Zr-1%Nb under tension and compression and calculated stress versus equivalent plastic strain of ultra-fine grained (UFG) and coarse grained (CG) Zr-1%Nb is shown in Figure 6.

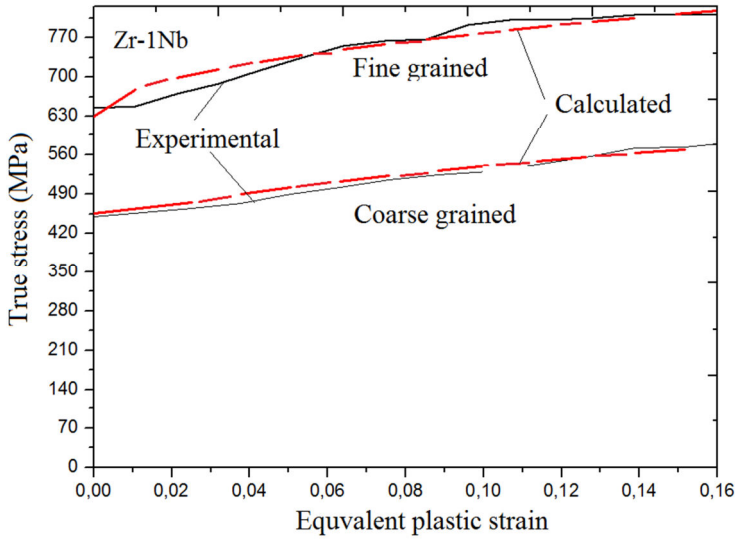

Fig. 6 - Calculated stress versus equivalent plastic strain of UFG and CG Zr-1%Nb

Solid curve corresponds to experimental data (Kazakov, 2015). Dashed curves were calculated by constitutive equation (2). The calculated stress-strain curves were obtained for UFG alloys taking into account changes of coefficient k_h in comparison with the value for GC alloys.

SUMMARY AND CONCLUSIONS

Mechanical behavior of Zr-1%Nb and Ti-13Nb-13Zr alloys was studied by numerical simulation method in practically important temperature range from 297 K to 1050 K.

Modified Johnson-Cook and Zerilli-Armstrong constitutive equations were used for numerical simulation mechanical behavior of Zr-Nb and Ti-Nb alloys with HCP and BCC phases.

It is shown that in order to obtain an adequate prediction of the flow stress of alloys experiencing eutectoid phase transformations, it is necessary to use different material parameters of Johnson-Cook model, within temperature range of the existence of alpha or beta phases.

At temperatures above the beta-phase transition temperature of Ti-Nb and Zr-Nb alloys it is advisable to use the constitutive equation Zerilli-Armstrong for BCC crystal structure

It was shown that the dependence of the normalized yield strength of Zr-1%Nb from normalized temperature can be approximated by a bilinear relation. The change in slope is due to phase transition $\alpha \rightarrow \beta$ (T~ 1070 K) in Zr-Nb alloys.

The effects of strain hardening and thermal softening were considered in the computational model.

Results of numerical simulation of quasi static loading of Zr-1%Nb and Ti-13Nb-13Zr alloys have a good agreement with experimental data.

The calculated stress-strain curves were obtained for UFG alloys taking into account changes in coefficient of the Hall-Petch relation in comparison with the value for GC alloys.

ACKNOWLEDGMENTS

This work was partially supported by the Russian Science Foundation (RSF), grant No. 16-1910264, the grant from the President of Russian Federation MK-2690.2017.8, and the grant from the Foundation of D. I. Mendeleev National research Tomsk State University within the program of increasing the competitiveness of TSU. The authors are grateful for the support of this research. Authors thank V. A. Serbenta for the help in work.

REFERENCES

[1] Abed F., Voyiadijs G.Z. A consistent modified Zerilli-Armstrong flow stress model for BCC and FCC metals for elevated temperatures//Acta Mechanica, 2005, 175(1), pp.1-18.

[2] Behera A.N., Chaudhuri A., Kapoor R., Chakravartty J.K., Suwas S. High temperature deformation behavior of Nb-1 wt.% Zr alloy // Materials & Design, 2016, 92, pp.750-759.

[3] Blokhin D. A., Chernov V.M., Blokhin A. I., Demin N. A., Sipachev I. V. Nuclear and physics properties of zirconium alloys E-110 and E-635 under long time neutron irradiation in the VVER-1000 reactor / D. A. Blokhin, // Advansed materials. - 2011, № 5, pp. 23-29.

[4] Bobbili R., Madhu V. Constitutive modeling and fracture behavior of a biomedical Ti-13Nb-13Zr alloy // Materials Science and Engineering A. 2017, 700, pp. 82-91.

[5] Bonisch M., Calin1 M., Waitz T., Panigrahi A., Zehetbauer M., Gebert A., Skrotzki W., Eckert J. Thermal stability and phase transformations of martensitic Ti-Nb alloys //Sci. Technol. Adv. Mater., 2013, 14, p. 055004 (9pp).

[6] Clouet E., Cottura M. Solubility in Zr-Nb alloys from first-principles //Acta Materialia, Elsevier, 2018, 144, pp. 21 - 30.

[7] Fong R.W.L. Anisotropic deformation of Zr-2.5Nb pressure tube material at high temperatures // Journal of Nuclear Materials. - 2013, 440, pp. 467-476.

[8] Gao C.Y., Zhang L.C., Yan H.X. A new constitutive model for HCP metals // Materials Science & Engineering A, 2011, pp. 4445-4452.

[9] Hatt B. A., Rivlin V. G. Phase transformations in superconducting Ti-Nb alloys // Journal of Physics D: Applied Physics, 1968, 1(9), pp. 1145-1149.

[10] Johnson G.R., Cook W.H. Fracture characteristics of three metals subjected to various strains, strain rates, temperatures and pressures // Eng. Fract. Mech., 1985, 21, pp. 31-48.

[11] Kazakov D. N., Kozelkov O. E., Mayorova A. S. Dynamic behavior of zirconium alloy E110 under submicrosecond shock-wave loading // EPJ Web of Conferences, 2015, 94, pp.1-5.

[12] Moffat D. L., Kattner U. R. Stable and metastable Ti-Nb phase diagrams // Metallurgical and Materials Transactions A 19, 1988, 10, pp. 2389-2397.

[13] Motta A.T., Yilmazbayhan A., Gomes da Silva M., Comstock R. J., Busby J., Gartner E. Zirconium alloys for supercritical water reactor applications: Challenges and possibilities // Journal of Nuclear Materials, 2007, 371, pp. 61-75.

[14] Nikonov A. Yu., Zharmukhambetova A. M., Skripnyak N. V., Ponomareva A. V., Abrikosov I. A., Barannikova S. A., and Dmitriev A. I. Calculation of mechanical properties of BCC Ti-Nb alloys // AIP Conference Proceedings, 2015, 1683 (020165).

[15] Rodchenkov B.S., Semenov A.N. High temperature mechanical behavior of Zr-2.5% Nb alloy// Nuclear Engineering and Design, 2005, 235, pp. 2009-2018.

[16] Sarkar A., Chandanshive S. A., Thota M. K., Kapoor R. High temperature deformation behavior of Zr-1Nb alloy // Journal of Alloys and Compounds, 2017, 703, pp. 56-66.

[17] Skripnyak N.V., Skripnyak V. A., Skripnyak V. V. Fracture of thin metal sheets with distribution of grain sizes in the layers // ECCOMAS Congress 2016 VII European Congress on Computational Methods in Applied Sciences and Engineering M. Papadrakakis, V. Papadopoulos, G. Stefanou, V. Plevris (eds.) Crete Island, Greece, 5-10 June 2016, 2016, 1, pp. 355-365.

[18] Skripnyak V.A., Skripnyak E.G. Mechanical behavior of nanostructured and ultrafine-grained metal alloy under intensive dynamic loading // Nanotechnology and Nanomaterials, (ed.) A. Vakhrushev, Chapter 2, 2017. ISBN 978-953-51-3182-3.

[19] Skripnyak V.A., Skripnyak N.V., Skripnyak E.G., Skripnyak V.V. Influence of grain size distribution on the mechanical behaviour of light alloys in wide range of strain rates //AIP Conference Proceedings 1793, 110001, 2017, 4p.

[20] Xiao D., Li Y., Hu S. High Strain Rate Deformation Behavior of Zirconium at Elevated Temperatures J. of Materials Science & Technology, 2010, 26, pp. 878-882.

[21] Zerilli F.J., Armstrong R.W. The effect of dislocation drag on the stress-strain behaviour of F.C.C. metals // Acta Metall. Mater, 1992, 40, pp. 1803-1808.